

## Light limitation of phytoplankton biomass and macronutrient utilization in the Southern Ocean

*B. Greg Mitchell*<sup>1</sup> and *Eric A. Brody*

Marine Research Division, Scripps Institution of Oceanography, UCSD,  
La Jolla, California 92093-0218

*Osmund Holm-Hansen*

Polar Research Program, Scripps Institution of Oceanography

*Charles McClain*

Goddard Space Flight Center, Code 970.1, Greenbelt, Maryland 20771

*James Bishop*

Lamont Doherty Geological Observatory of Columbia University,  
Palisades, New York 10964

### *Abstract*

The Antarctic Circumpolar Current (ACC) is unique in that it has continually high concentrations of major plant nutrients but low phytoplankton biomass. This enigmatic phenomenon is the focus of significant speculation that trace nutrients, including Fe, may limit phytoplankton crop size.

Global climatologies indicate that the ACC is a region with low surface temperatures, weak density stratification, little summertime surface solar irradiance, and strong wind stress. These physical phenomena act to limit growth rates of the phytoplankton community. Using a photo-physiological description of phytoplankton growth in a simple one-dimensional ecosystem model forced by observations or climatologies of mixing depth and surface irradiance, we make an evaluation of the potential for massive, nutrient-exhausting, phytoplankton blooms forming in the ACC. The ACC has persistent mixed layers in excess of 50 m. Literature values and model optimization indicate that the minimal aggregate specific loss rate for phytoplankton, including respiration, sinking, and grazing, is  $\sim 0.2 \text{ d}^{-1}$ . For a minimal loss rate and typical physical conditions of stratification and surface irradiance, the model predicts that phytoplankton in the ACC would not utilize > 10% of the available macronutrients. Without a mechanism for increasing the strength of stratification, we predict that massive Fe additions to the Southern Ocean would fail to significantly mitigate the atmospheric  $\text{CO}_2$  derived from fossil fuel.

---

<sup>1</sup> Corresponding author.

### *Acknowledgments*

We acknowledge the organizers of the American Society of Limnology and Oceanography symposium for which this paper was prepared. In particular, the efforts of Susan Weiler, Penny Chisholm, John Cullen, and François Morel are acknowledged. Our colleagues in the RACER program are also acknowledged, in particular the captain and crew of RV *Polar Duke*, and Anthony Amos who provided the hydrographic and beam attenuation data from RACER 2. Vincent Spode provided technical assistance with graphics. We are grateful to H. Sosik, D. Nelson, R. Anderson, R. Sambrotto, and two anonymous reviewers for comments on drafts of the manuscript.

This research was supported by various grants from the NSF Division of Polar Programs and from NASA. The manuscript was prepared while B. G. Mitchell was a visiting senior scientist at the Jet Propulsion Laboratory of California Institute of Technology, on detail to NASA Headquarters as program scientist for ocean biogeochemistry.

Contribution 4815 from Lamont Doherty Geological Observatory.

The Southern Ocean and the Antarctic Circumpolar Current (ACC) south of the polar front comprise  $\sim 10\%$  of the world's ocean surface (El Sayed 1978) and contain significant concentrations of surface macronutrients (i.e.  $\text{NO}_3$ ,  $\text{PO}_4$ ,  $\text{SiO}_4$ ). There has been extensive speculation on the proximate cause of phytoplankton biomass limitation, which prevents complete depletion of surface macronutrients. In a paper on Antarctic phytoplankton ecology, Hart (1934) discussed several potential reasons for the lack of nutrient utilization including seasonal light, grazing, physical mixing, and Fe limitation. These concepts, singly or in combination, have been expanded upon and elaborated over the years and have been reviewed previously (Holm-Hansen et al. 1977; El-Sayed 1987).

An intriguing hypothesis has been posited

(Martin et al. 1990a,b; Martin 1990); it states that Fe fertilization of the Southern Ocean would promote a bloom sufficient to remove from the atmosphere substantial amounts of the CO<sub>2</sub> derived from fossil fuel. Martin's hypothesis is based on two observations. First, the absolute concentrations of trace nutrients (i.e. Fe) in open-ocean Antarctic waters are low relative to NO<sub>3</sub> and other macronutrients (Martin et al. 1990b; de Baar et al. 1990). Second, experiments in which uncontaminated Antarctic near-surface waters were enclosed in bottles subjected to high light and additional Fe resulted in rapid growth of some of the phytoplankton present and complete utilization of the available macronutrients (i.e. NO<sub>3</sub>) (de Baar et al. 1990; Martin et al. 1990a; Buma et al. 1991). Compelling ancillary observations that support the iron hypothesis include evidence that the ACC has one of the lowest fluxes of atmospheric dust (Duce 1986) and the inverse correlation over the last 100,000 yr between Al dust (a proxy for Fe and other trace elements in atmospheric dust) and atmospheric CO<sub>2</sub> in Antarctic ice cores (De Angelis et al. 1987; Martin 1990).

The experiments of Martin et al. (1990a) did not allow a test of light vs. trace metal limitation, although light has often been suggested as a controlling factor for Antarctic phytoplankton growth rates (Hart 1934; Holm-Hansen et al. 1977; Smith and Nelson 1985; Sakshaug and Holm-Hansen 1986; Mitchell and Holm-Hansen 1991a). Mixing, stratification, the availability of light for phytoplankton growth, and modeling of these have been studied extensively (e.g. Gran and Braruud 1935; Ryther and Yentsch 1957; Cushing 1962; Steele 1962; Steele and Menzel 1962; Platt et al. 1977). Our objective here is to apply these concepts to the issue of phytoplankton biomass accumulation and nutrient utilization in the Southern Ocean.

Antarctic blooms have been observed only where stratification provided a favorable light regime. Smith and Nelson (1985) reported that Antarctic ice-edge blooms exhibited strong coherence with the density field, ostensibly due to a more favorable light regime compared to the adjacent deeply mixed open waters. Development of mas-

sive blooms ( $>10$  mg Chl *a* m<sup>-3</sup>) has been documented in coastal waters with strong stratification (Mandelli and Burkholder 1966; Holm-Hansen et al. 1989; Holm-Hansen and Mitchell 1991). By contrast, deeply mixed coastal waters did not exhibit an ability to develop massive blooms (Holm-Hansen and Vernet 1990; Mitchell and Holm-Hansen 1991a). NO<sub>3</sub> exhaustion has been reported for ice-edge (Nelson and Smith 1986) and coastal blooms (Holm-Hansen et al. 1989).

The classic concepts presented by Sverdrup (1953) have recently been revisited for the Antarctic by Mitchell and Holm-Hansen (1991a) and Nelson and Smith (1991). A more general review was given by Smetacek and Passow (1990). A fundamental parameter, the "critical depth" ( $Z_c$ ), is the mixing depth that results in no net phytoplankton community growth. If phytoplankton sustained no loss, deep mixing would slow phytoplankton growth rates, but over a growth season, a bloom could still develop. Indeed, if the only loss was a specific respiration rate of 0.1 d<sup>-1</sup>, Yentsch (1981) pointed out that  $Z_c$  would be as deep as 700 m for typical temperate phytoplankton growing in relatively transparent water. However, to evaluate community biomass accumulation and utilization of nutrients, one must consider losses due to respiration, sinking, grazing, and advection (Smetacek and Passow 1990). Through modeling of reasonable scenarios of mixing and phytoplankton loss, one can evaluate the potential phytoplankton biomass (and nutrient utilization). In this paper, we use a simple one-dimensional ecosystem model to evaluate potential phytoplankton biomass and surface nutrient utilization in the Southern Ocean.

### Methods

*Hydrography and water samples*—Data from three Antarctic cruises form the basis for development and parameterization of a model of light-dependent phytoplankton growth. During the Vulcan 6 cruise on RV *Melville* studies of the hydrography and phytoplankton distributions in the Scotia Sea were carried out. Density fields were determined with a Neil Brown CTD system

and water samples were collected with a General Oceanics Rosette equipped with 10-liter bottles. Details of the analyses for density and pigments are given by Foster and Middleton (1984) and Biggs et al. (1982).

As part of the Research on Antarctic Coastal Ecosystem Rates (RACER) program, two cruises to the Bransfield and Gerlache Straits on the RV *Polar Duke* were accomplished in the 1986–1987 austral summer (RACER 1) and from October to November 1989 (RACER 2). At each station during RACER 1 a profiling system was deployed between the surface and 200 m for continuous recording of physical, optical, and biological parameters. This profiling unit consisted of a General Oceanics rosette equipped with the sensors listed below and ten 10-liter PVC Niskin bottles with teflon-covered springs. Sensors on the profiling unit included temperature and conductivity (Sea Bird Electronics, Inc.), a 0.25-m path-length transmissometer (Sea Tech, Inc.), a flash-lamp fluorometer (Sea Tech, Inc.), and a MER 1012-F optical unit (Biospherical Instr., Inc.) for recording depth, photosynthetically available light (PAR), seven channels of downwelling spectral irradiance, and five channels of upwelling spectral radiance.

During RACER 2, station A (64°12.8'S, 61°19.3'W) was occupied 5 times between early October and late November. The CTD data during this cruise were collected with a Sea Bird, Inc., system that included a General Oceanics, Inc., rosette with 10-liter bottles and a 25-cm path-length transmissometer (Sea Tech, Inc.), but no other optical instruments. The transmissometer data were converted to the beam attenuation coefficient ( $c_t$ ,  $m^{-1}$ , Bartz et al. 1978). Argos-tracked water-mass drogues were deployed to define the flow fields. Details of the RACER 2 study of spring bloom development mechanisms can be found elsewhere (Huntley et al. 1990).

Water samples for Chl *a* and pheopigments (pheo) analysis (50–100 ml) were filtered at a vacuum differential of <20 cm of Hg through 25-mm glass-fiber filters (Whatman GF/F). Pigments on the filters were extracted in absolute methanol (Holm-Hansen and Riemann 1978) and the Chl *a* and pheopigment concentrations were de-

termined by measuring fluorescence (Holm-Hansen et al. 1965) in a Turner Designs fluorometer. The fluorometer was calibrated against HPLC purified Chl *a*. Stability of the calibration was checked daily with a coproporphyrin standard (COP-I-5, Sigma Chem. Co.). Nutrients collected from the water sampler during RACER 2 were determined with a Technicon II AutoAnalyzer and standard colorimetric methods (Strickland and Parsons 1972).

*Global imagery*—Global climatologies of wind stress (Trenberth et al. 1990), satellite-derived surface irradiance (Bishop and Rossow 1991) and Coastal Zone Color Scanner (CZCS) surface pigments (Feldman et al. 1989) were mapped to a common projection and output as color images using the Ocean Computing Facility at Goddard Space Flight Center.

*Model of light-dependent production*—A simple model of light-dependent photosynthesis was developed based on empirical observations from RACER 1. Detailed descriptions of the model (Mitchell and Holm-Hansen 1991a), in situ primary production (Holm-Hansen and Mitchell 1991), and pigment-specific light attenuation coefficients (Mitchell and Holm-Hansen 1991b) have been published elsewhere. The list of notation summarizes the definitions of symbols and parameters used here and Table 1 summarizes the fundamental equations of the model. Nutrient limitation of phytoplankton growth rate is not included because our objective is to understand the light limit of phytoplankton biomass and nutrient utilization assuming all nutrients are in excess of concentrations required for maximal growth.

The accumulation of Chl *a* biomass through time ( $t$ ) is described by Eq. 1 where  $[Chl\ a]_0$  and  $[Chl\ a]$  are the initial and final concentrations of Chl *a* over some time increment  $t$ . The difference between specific growth and loss rates of phytoplankton biomass,  $\mu$  and  $l$ , determines the rate of accumulation or decline in the crop. The value of  $l$  is the sum of losses due to respiration ( $R$ ), grazing ( $I_g$ ) and sinking ( $I_s$ ). In this simple model, the loss terms are aggregated and held constant during model runs.

The C-based rate of primary production

Notation	
$\alpha$	Chl <i>a</i> -specific initial slope of <i>P</i> - <i>I</i> relationship
C:Chl <i>a</i>	Ratio of C:Chl <i>a</i> for phytoplankton (wt/wt)
C:N	Molar ratio of phytoplankton C:N
[Chl] <sub>0</sub> , [Chl] <sub><i>t</i></sub>	Chl <i>a</i> concentration at time 0 and time <i>t</i>
<i>c<sub>t</sub></i>	Beam attenuation coefficient
<i>d</i> Chl <i>a</i>	Daily change in Chl <i>a</i> concentration of UML
$\mu$	Specific growth rate of phytoplankton
<i>l</i>	Specific loss rate of phytoplankton
<i>l<sub>g</sub></i>	Specific rate of grazing
<i>l<sub>s</sub></i>	Specific rate of phytoplankton sinking
<i>K<sub>PAR</sub></i>	Diffuse attenuation coefficient for PAR
<i>k<sub>z</sub></i>	Vertical diffusivity coefficient
[NO <sub>3</sub> ], [NO <sub>3</sub> ] <sub><i>i</i></sub>	NO <sub>3</sub> concentration, initial NO <sub>3</sub> concentration
<i>P<sub>m</sub></i>	Maximum Chl <i>a</i> -specific rate of photosynthesis
<i>P<sub>C</sub></i>	Hourly rate of C production
<i>P<sub>C</sub></i> (UML)	Daily mean C production of UML
PAR	Photosynthetically available radiation
PAR(0 <sup>+</sup> )	Downwelling PAR at the sea surface
<i>R</i>	Specific rate of phytoplankton respiration
$\tau$	Light transmittance of the air-sea interface
UML	Upper mixed layer of the ocean
<i>z</i>	Depth in the ocean
<i>Z<sub>UML</sub></i>	Depth of the UML
<i>Z<sub>c</sub></i>	critical <i>Z<sub>UML</sub></i> for zero net phytoplankton growth

$P_C$  (mg C m<sup>-3</sup> h<sup>-1</sup>) at any depth *z* in the upper mixed layer (UML) is determined with Eq. 2. This model of production follows the formulation of Platt and Jassby (1976). The parameterization of Holm-Hansen and Mitchell (1991), based on > 140 in situ production measurements, was used for  $\alpha$  [0.06 mg C (mg Chl *a*)<sup>-1</sup> h<sup>-1</sup> ( $\mu$ Einst m<sup>-2</sup> s<sup>-1</sup>)<sup>-1</sup>] and  $P_m$  [1.1 mg C (mg Chl *a*)<sup>-1</sup> h<sup>-1</sup>], which are the initial slope and maximum rate of the Chl *a* specific photosynthesis-irradiance relationship.

PAR(*z*), the photosynthetically available radiation at depth *z*, is calculated with Eq. 3, where PAR(0<sup>+</sup>) is the flux of PAR above the sea surface. The value of  $\tau$  was assumed to be 0.8, representing both surface transmittance and rapid absorption of red light

Table 1. Fundamental equations used in the one-dimensional model.

$[\text{Chl } a]_t = [\text{Chl } a]_0 \exp(\mu - l)t$	(1)
$P_C(z) = [\text{Chl } a]_0 P_m \{1 - \exp(-[\alpha \text{PAR}(z)/P_m])\}$	(2)
$\text{PAR}(z) = \text{PAR}(0^+) \tau \exp(-K_{\text{PAR}}z)$	(3)
$K_{\text{PAR}} \text{ (m}^{-1}\text{)} = 0.078 + 0.0136 \cdot [\text{Chl } a + \text{pheo (mg m}^{-3}\text{)}]$	(4)
$d\text{Chl } a = P_C(\text{UML})/\text{C:Chl } a$	(5)
$\mu \text{ (d}^{-1}\text{)} = \ln\{([\text{Chl } a]_0 + d\text{Chl } a)/[\text{Chl } a]_0\}$	(6)
$l = R + l_s + l_g$	(7)

in the top few meters (Austin 1974). The attenuation coefficient for PAR in the mixed layer,  $K_{\text{PAR}}$ , is well correlated to pigment concentrations as shown by Eq. 4 (linear fit,  $r^2 = 0.74$ ,  $n = 130$ ). Equation 4, the least-squares best-fit to the observations, is used in the model.

Pheopigments are not explicitly included in the model; it is assumed that the attenuation coefficient of Chl *a* is similar to observed attenuation by Chl *a* + pheo. We only model the response of the UML, where Chl *a* is constant with depth, so  $K_{\text{PAR}}$  is assumed to have no depth dependence. The surface irradiance, PAR(0<sup>+</sup>) was estimated from the satellite-derived irradiance method of Bishop and Rossow (1991).

The daily change in Chl *a* concentration in the UML, *d*Chl *a*, is calculated according to Eq. 5 where  $P_C(\text{UML})$  is the daily mean C-based productivity over the entire mixed layer at the end of a growth day. The assumption that the UML has a uniform distribution of Chl *a* at the end of a growth day in spite of differential light-dependent rates of growth is justified based on the uniform vertical profiles of particulates typically observed in the UML (e.g. Mitchell and Holm-Hansen 1991a). The phytoplankton (Chl *a*) specific growth rate for the UML can then be calculated with Eq. 6.

From the equations in Table 1, it is evident that the specific growth rate of the phytoplankton in the UML will be a function only of the surface irradiance, depth of mixing, C:Chl *a*, and concentration of Chl *a* in the mixed layer. Loss terms (Eq. 7) were applied at the end of each growth day so that *d*Chl *a* could be used to calculate the

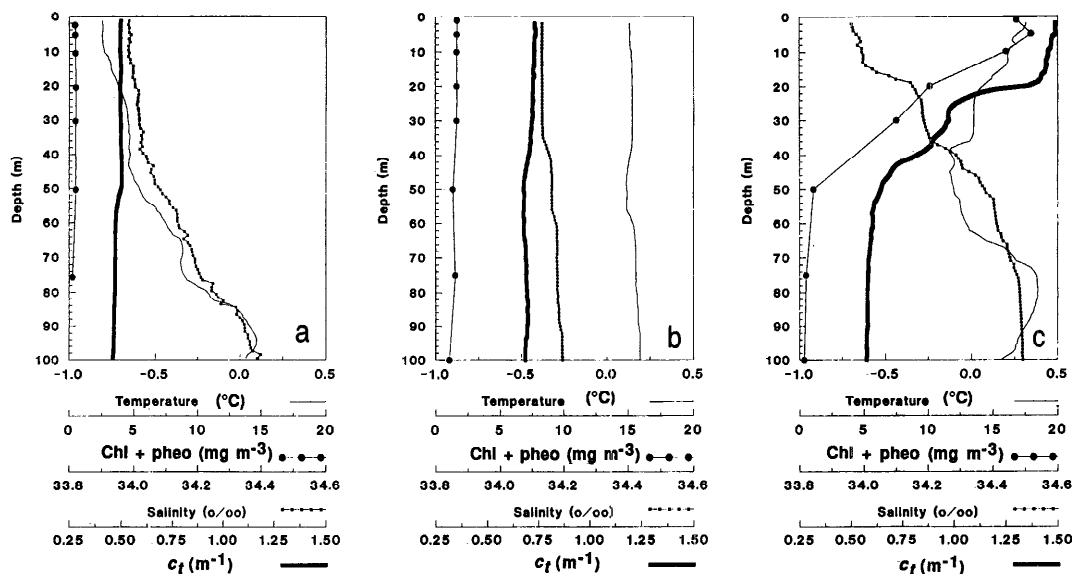


Fig. 1. Vertical profiles of hydrographic (temperature and salinity) and phytoplankton biomass (Chl *a* and beam attenuation coefficient,  $c_f$ ) parameters in the Gerlache Strait in austral spring 1989. [a.] RACER 2, station A, 10 October 1989. [b.] RACER 2, station FC08, 15 November 1989. Station FC08 was ~50 km from station A in the western portion of Bransfield Strait. [c.] RACER 2, station A, 17 November 1989. Note the shallow mixed layer and the associated massive bloom at station A in late November.

specific growth rate. During runs of the model *l* was held constant.

For all runs, the molar ratio of C : N (mol/mol) was 6.6 (Redfield et al. 1963). Values on C : N of 7–8 have been reported for Antarctic waters (Nelson et al. 1989; Holm-Hansen et al. 1989), although detrital material may be partially responsible for values higher than those expected for phytoplankton. The initial  $\text{NO}_3$  concentration ( $[\text{NO}_3]_i$ ) of  $30 \text{ mmol m}^{-3}$  was the typical value below 100 m during RACER 2. The initial Chl concentration was  $0.1 \text{ mg m}^{-3}$ , which is typical of winter and early-spring conditions in the Antarctic (Clark et al. 1988; Brightman and Smith 1989). Maximum specific growth rates predicted by the model were  $0.42 \text{ d}^{-1}$ , which is in good agreement with estimates in the literature (Wilson et al. 1986; Sakshaug and Holm-Hansen 1986; Tilzer and Dubinsky 1987; Spies 1987). The *f*-ratio, which is the fraction of the total production that is based on  $\text{NO}_3$ , was held at 0.5 for all runs of the model. This number is typical of observations in the Antarctic (Olson 1980; Glibert et al. 1982; Koike et al. 1986; Smith and Nelson 1990).

## Results and discussion

**Spring bloom at station A**—During RACER 2 mixed-layer depths at station A were persistently shallow (<20 m) after early November (Holm-Hansen and Vernet 1990). Waters only 40 km away were in a dynamic flow field and maintained deep mixed layers (>40 m). Station A, with shallow mixed layers, developed a massive bloom whereas the more deeply mixed waters nearby did not (Fig. 1b,c). The Gerlache Strait has been reported to have excess trace metals, including Fe (Martin et al. 1990b), so the minimal bloom at FC08 (Fig. 1b) is likely a consequence of deeper mixing in the region preventing phytoplankton growth rates from exceeding loss rates.

A time series at station A reveals a classic spring bloom (Fig. 2). The mixed layer shoaled from >40 m in early October to <10 m during the second half of November (days 284–324, Fig. 2a). During this period, mixed-layer  $\text{NO}_3$  was reduced from  $30 \text{ mmol m}^{-3}$  to ~5 (Fig. 2b). This nutrient depletion was caused by a massive bloom of phytoplankton that attained a maximum

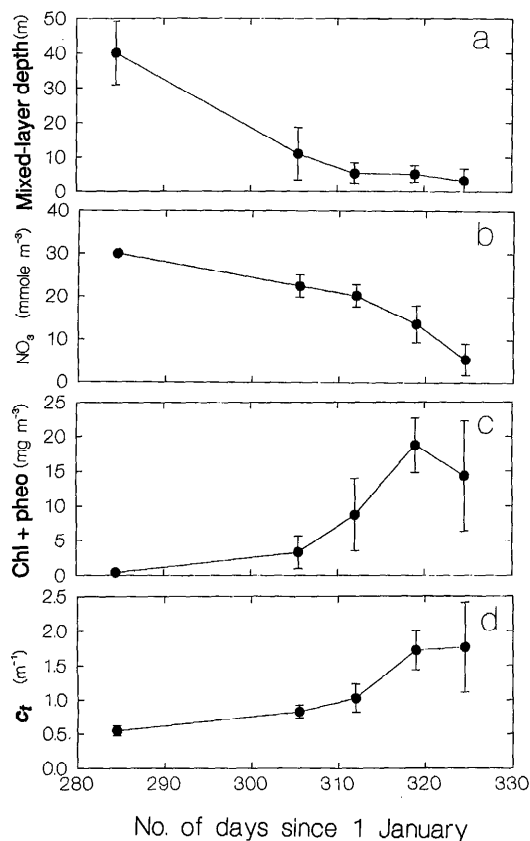


Fig. 2. Time series of several variables at RACER 2, station A, during the 1989 spring bloom. [a.] Mixed-layer depth. [b.]  $\text{NO}_3$  concentration in the UML. [c.] The sum of Chl *a* + pheopigments in the UML. [d.] The beam attenuation coefficient ( $c_t$ ) in the UML.

value of  $>15 \text{ mg Chl } a + \text{ pheo m}^{-3}$  around 16 November (day 320, Fig. 2c). The bloom was also easily followed optically with the transmissometer to determine beam attenuation coefficients (Fig. 2d).

The results of the drogue study indicated that station A was located in an isolated water mass that maintained its integrity from early November 1989 through January 1990 (Niiler et al. 1990). A drogue released in the vicinity of station A made repeated circles for 3 months with a radius of  $\sim 15 \text{ km}$ . The drogue motion, implying a topographically trapped eddy, justifies use of the simple one-dimensional model of Mitchell and Holm-Hansen (1991a).

**Model evaluation for the station A time series**—The time series of  $\text{NO}_3$  utilization

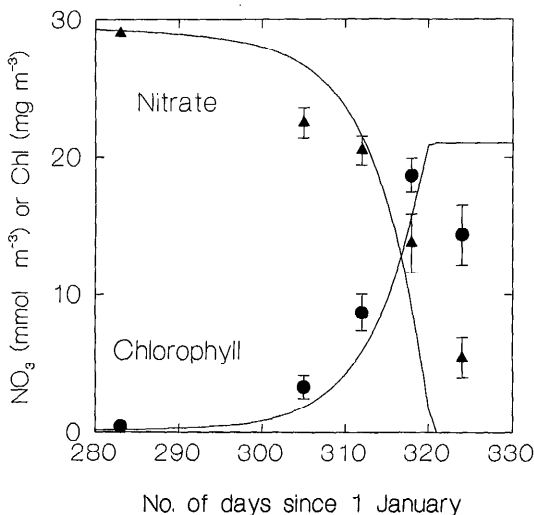


Fig. 3. Comparison of model results with observations for  $\text{NO}_3$  and Chl *a* at RACER 2, station A, for the time series presented in Fig. 9. The best-fit of the model was achieved with  $l = 0.27 \text{ d}^{-1}$ .

and phytoplankton growth at station A during RACER 2, shown in Fig. 2b,c, is useful for parameterization and testing of the temporal predictions of the one-dimensional ecosystem model. The observed values of  $Z_{\text{UML}}$  at station A were used to force the model. Mixing depths were linearly interpolated between observations (as diagrammed in Fig. 2a). The irradiance time series for  $55^\circ\text{S}$ ,  $130^\circ\text{W}$  (see Fig. 9b), estimated with the method of Bishop and Rossow (1991), was used to force the model.

With the constraints described above, the only free parameter in the model is the loss rate. The best-fit to the RACER 2 observations was obtained with  $l = 0.27$  (Fig. 3). For this set of parameter values, modeled chlorophyll pigments at station A attain a maximum of  $\sim 20 \text{ mg m}^{-3}$  when  $\text{NO}_3$  is exhausted. In the model, it is assumed that the phytoplankton crop cannot increase in size once  $\text{NO}_3$  is exhausted. The model agrees very well with pigment and  $\text{NO}_3$  data up to 16 November (day 320). On 21 November (day 325) observed pigments are lower than the model predicts and  $\text{NO}_3$  has not been exhausted as in the model, which is consistent with the fact that  $\text{NH}_4$  is an effective inhibitor of  $\text{NO}_3$  uptake for Antarctic phytoplankton (Olson 1980; Glibert

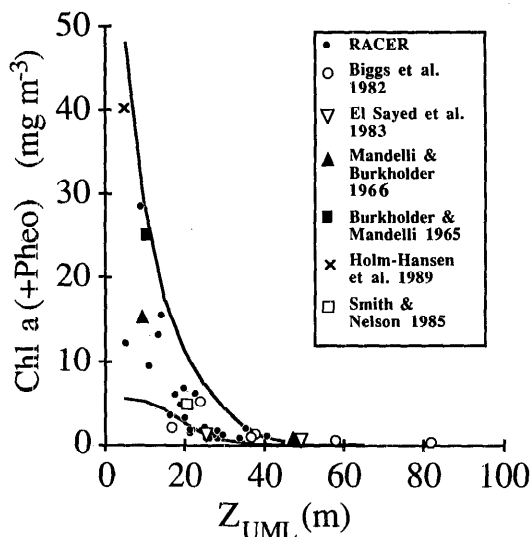


Fig. 4. Observations and modeling of the Antarctic phytoplankton crop in relation to mixed-layer depth (from Mitchell and Holm-Hansen 1991a). The observations are bounded by model runs with specific loss rates between  $0.3$  and  $0.35 \text{ d}^{-1}$  (solid lines).

et al. 1982; Koike et al. 1986).  $\text{NH}_4$  concentrations at station A ranged from  $0.6$  to  $2.0 \text{ mmol m}^{-3}$  after 1 November (day 305) (Holm-Hansen et al. 1990). As argued by Mitchell and Holm-Hansen (1991a) one does not expect exhaustion of  $\text{NO}_3$  if  $\text{NH}_4$  is present, due to inhibition of  $\text{NO}_3$  utilization and the continual resupply of  $\text{NO}_3$  via vertical diapycnal transport. Because the model does not include an explicit term for competitive inhibition of  $\text{NO}_3$  uptake by  $\text{NH}_4$ , it is not surprising that it fails to predict nutrient values in the period after the peak bloom.

**Model evaluation for diverse Antarctic ecosystems**—Mitchell and Holm-Hansen (1991a) applied the model in an evaluation of observations of  $Z_{\text{UML}}$  and Chl *a* concentrations in the UML for diverse Antarctic ecosystems. They concluded that  $Z_{\text{UML}}$ , which together with biomass and surface irradiance controls the mean irradiance within the UML, may be an important determinant of the potential size of the Antarctic phytoplankton crop (Fig. 4). Their model was used to estimate the loss rate for Antarctic phytoplankton that would be required for the model to match the obser-

vations, assuming nutrients were unlimited. A model loss rate between  $0.3$  and  $0.35 \text{ d}^{-1}$  provided the best-fit to observations. The data embodied in Fig. 4 do not provide conclusive proof of a causal relationship between depth of mixing and size of the crop. For example, open-ocean regions with deep mixed layers are also regions expected to have the lowest concentrations of trace nutrients. The model alone may not be able to define precisely the limit of the phytoplankton crop size. However, agreement in the loss rate parameter of the model required to fit independent data sets (Figs. 3, 4) provides some added measure of confidence that the model can help evaluate the relationship between available light and nutrient utilization.

**Chlorophyll and stratification in the Scotia Sea**—During the Vulcan 6 cruise, a transect of the density structure in the Scotia Sea, along  $38^\circ 5' \text{E}$ , from the southern Scotia Ridge to South Georgia Island reveals that the region from  $55$  to  $57^\circ \text{S}$  is characterized by mixed layers  $> 50 \text{ m}$  in January (Fig. 5a). Shallower mixed layers and stronger stratification were observed north of  $55^\circ \text{S}$  and south of  $59^\circ \text{S}$ . Significantly, higher Chl *a* concentrations were observed in the regions with stronger and shallower stratification (Fig. 5b). This region may have relatively high concentrations of trace metals (Martin et al. 1990b; de Baar et al. 1990). Nevertheless, in midsummer 1981, Chl *a* in the UML along this transect did not exceed  $1.0 \text{ mg Chl a m}^{-3}$  except over the shelf areas near the Scotia Ridge and South Georgia Island. Maximum values near South Georgia Island were  $3 \text{ mg Chl a m}^{-3}$ .  $\text{NO}_3$  in the UML during this transect was never  $< 16 \text{ mmol m}^{-3}$  (Biggs et al. 1982). If trace metal or Fe fertilization were to be considered as a viable means of atmospheric  $\text{CO}_2$  remediation, substantially higher biomass and greater nutrient depletion would be necessary in the vast portions of the ACC that are similar to the open-ocean regions shown in Fig. 5.

**Climatologies of the ACC**—The most fundamental physical-chemical parameters for phytoplankton growth are temperature, nutrient concentrations, depth of physical mixing, and amount of solar radiation at

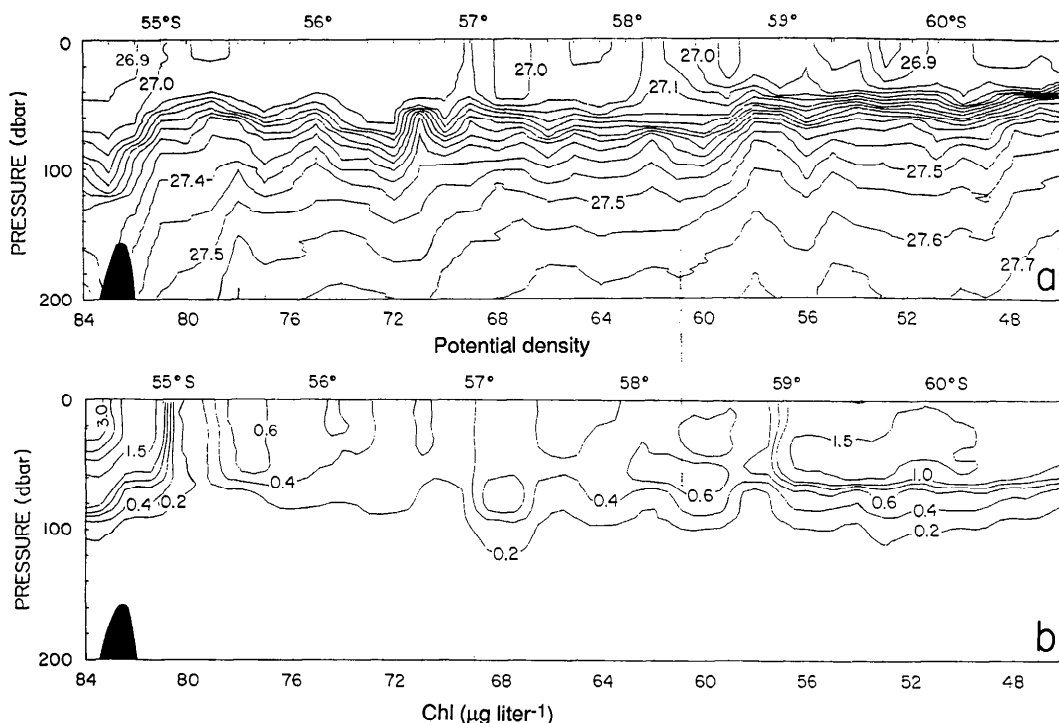


Fig. 5. Vertical sections for transect 4 (38°S) of Vulcan expedition in the Scotia Sea, February 1981. Numbers below each figure represent station numbers; latitude is indicated above each figure. [a.] Potential density ( $\sigma_t$ ). [b.] Chl *a* concentrations in the upper 200 m.

the surface. In the ACC, temperatures range from  $-2^{\circ}\text{C}$  to  $+4^{\circ}\text{C}$ —among the lowest in surface waters on earth. Thermodynamic constraints of fundamental cellular biochemistry result in a low maximal growth rate for species that can grow at these temperatures (Eppley 1972; Neori and Holm-Hansen 1982; Priscu et al. 1989). Nutrients previously have been considered abundant, due to the very high concentrations of macronutrients such as  $\text{NO}_3$ ,  $\text{PO}_4$ , and  $\text{SiO}_4$  in the region of interest (Hart 1934, Holm-Hansen et al. 1977). High levels of surface nutrients are not surprising considering the climatology of ocean density that reveals nearly vertical isopycnals in the ACC (Fig. 6). The ACC efficiently exchanges water between the surface and the nutrient-rich deep ocean. This “window” to the deep ocean affords luxuriant surface macronutrients; it must also be viewed as a mechanism for deeply mixing the phytoplankton community.

Even with apparent luxuriant surface macronutrients, biomass and primary production of the Southern Ocean are relatively low (Hart 1934; Holm-Hansen et al. 1977; El-Sayed et al. 1983; Nelson and Smith 1986) leading to the conclusion by El-Sayed (1987) that this enigmatic situation is the “paradox” of the Southern Ocean. The low phytoplankton biomass ( $0.1\text{--}2\text{ mg m}^{-3}$ ) throughout the ACC has been substantiated by satellite-derived pigment distributions (Fig. 7a), although coastal and ice-edge regions do indicate blooms. It should be noted that the 7-yr mean pigment field from the CZCS presented in Fig. 7a is comprised only of data collected during spring and summer. This period is well lighted and corresponds to the seasons of maximal primary production and phytoplankton crop size.

The region is unique in another way: the strongest surface wind stresses of the world ocean are observed there (Fig. 8a). The stresses have maximal values in July and



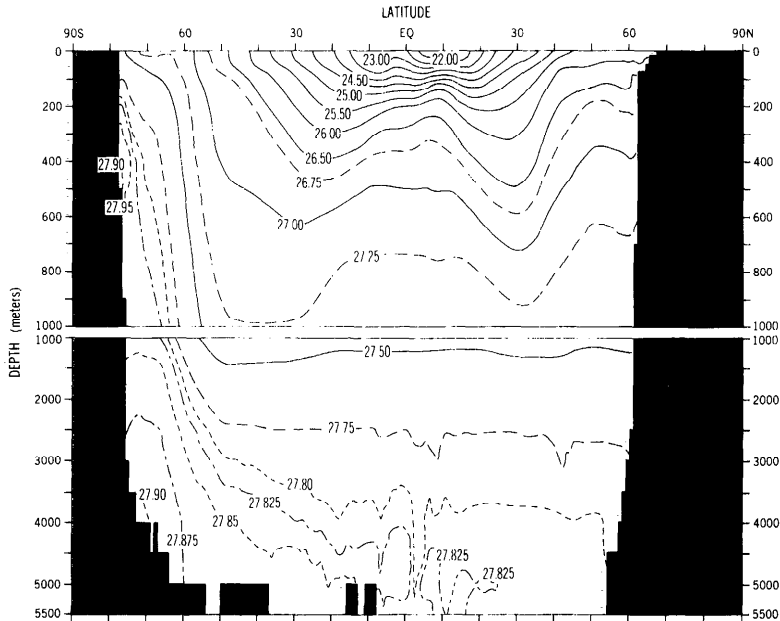


Fig. 6. Climatological density structure of the Pacific Ocean basin (from Levitus 1982).

August and minimal values in December and January with peak austral winter values being 50% greater than peak summer values (Trenberth et al. 1990). The climatological data on density structure (Fig. 6) and wind stress (Fig. 8a) and theoretical relationships (e.g. Kraus and Turner 1967; Denman 1973; Denman and Miyake 1973; Niiler 1975) lead to the conclusion that the Circumpolar Current should have among the deepest surface mixed layers. Indeed this has been shown to be the case (Levitus 1982). Based on observed density and typical winds, Mitchell and Holm-Hansen (1991a) concluded that open waters of the Drake Passage would stay continually mixed to depths of at least 40–50 m, which is consistent with observations in the Scotia Sea (Fig. 5a; Nelson and Smith 1991). Knowledge of actual  $Z_{\text{UML}}$  in the ACC is limited, and no true time series is available. Lacking a true  $Z_{\text{UML}}$  time series,  $Z_{\text{UML}}$  was held constant during runs of the model.

A final unique feature of the physical climatology of the Circumpolar Current is that the region experiences the lowest summer surface irradiance of any region on earth (Bishop and Rossow 1991; Fig. 8b). Low solar energy minimizes thermal stratifica-

tion and light-limited growth rates. The Scotia Sea, from the South Shetland Islands in the southwest to South Georgia Island in the northeast, has relatively high light and low wind stress (Fig. 8). Satellite imagery reveals that this regime has the highest surface pigments of the ACC (Fig. 7a). J. Martin (pers. comm.) argues that this region also has relatively high trace metals due to transport off the Antarctic Peninsula shelf into the Weddell-Scotia confluence. There are compelling reasons to examine the unknown environmental mechanism(s) causing the biomass difference southeast and southwest of South Georgia Island.

The zonal mean irradiance in the vicinity of 55–60°S, 130°W for January 1984 is the lowest southern hemisphere irradiance in summer (Fig. 9a). The satellite-derived time series of irradiance at 55°S for 1983–1984 is shown in Fig. 9b compared to the clear-sky irradiance. Persistent clouds over the ACC are a significant factor limiting the irradiance required for bloom formation.

*Applications of the model to the ACC*—The climatological data and ecosystem model described above allow assessment of the potential for the ACC to develop massive, nutrient-depleting, phytoplankton

blooms. An evaluation of varying both  $Z_{\text{UML}}$  and  $l$  is shown in Fig. 10. In this analysis, the irradiance used was from the satellite-derived results of Bishop and Rossow (1991; Fig. 9b) for 55°S, 130°W. The value of Chl  $a$  for 31 December (day 365, midsummer) is plotted. Experimental data on respiration (Tilzer and Dubinsky 1987), sinking (Johnson and Smith 1986) and grazing (Huntley et al. 1991; Mitchell and Holm-Hansen 1991a), and previous model parameterizations (Mitchell and Holm-Hansen 1991a; Fig. 3) lead to the inevitable conclusion that a minimal loss term is between  $l = 0.15$  and  $0.25 \text{ d}^{-1}$ . For  $l = 0.2 \text{ d}^{-1}$  and a mixed layer of 50 m, the midsummer Chl  $a$  concentration attained is only  $5 \text{ mg Chl } a \text{ m}^{-3}$  (Fig. 10).

Although the model predicts a potential crop size (with minimal loss rates) greater than typical ACC observations (but consistent with maximum values in the ACC observed with the CZCS), such blooms would fall far short of total nutrient utilization. If we assume a vertical diffusion coefficient for  $\text{NO}_3$  transport of  $k_z = 5 \times 10^{-5} \text{ m}^2 \text{ s}^{-1}$ , only  $\sim 10\%$  of surface nutrients are predicted to be utilized. This value of  $k_z$  is consistent with previous observations (Denman and Gargett 1983; Gregg 1987), is similar to the rate assumed by Peng and Broecker (1990), and agrees with model estimates by Mitchell and Holm-Hansen (1991a). The actual fraction of nutrients used will be extremely dependent on the true value of  $k_z$  and the  $f$ -ratio. Although a reasonable range for the magnitude of the  $f$ -ratio can be estimated from literature data, there is a complete lack of instantaneous estimates of  $k_z$  measurements in the Antarctic. Such data are crucial for any final modeling evaluation of the potential for Antarctic phytoplankton to utilize the available nutrients. If actual grazing losses are greater or mixed layers deeper than these minimum estimates, the probability of significant nutrient removal would be even less likely. Nelson and Smith (1991) have come to a similar conclusion.

Without shallow mixed layers ( $< 30 \text{ m}$ ) it is unlikely that the phytoplankton crop could utilize all available nutrients as has been modeled in the long-term global  $\text{CO}_2$  abatement scenarios that have been proposed

(Sarmiento and Siegenthaler 1991; Peng and Broecker 1990). The concept of a critical mixing depth that limits bloom formation is not novel (e.g. Sverdrup 1953) but must be considered for a thorough evaluation of the true limit of phytoplankton nutrient utilization.

The model used here is admittedly simple. It does not include a dynamic mixed layer, variable grazing pressure, explicit nutrient competition, or advective transport. Although it could be argued that this approach is overly simplistic, we believe it is arbitrary to explicitly model components of the system for which there are few observational data. The in situ photosynthesis-irradiance and pigment-specific attenuation coefficients are well described and based on extensive Antarctic observations.

Rather than arbitrarily model other parameters (mixing depth, grazing, sinking and respiration losses, etc.), we prefer to perform sensitivity analysis of the model with these terms and evaluate the results for reasonable scenarios. Reasonable bounds for respiration (e.g. Tilzer and Dubinsky 1987) and sinking (e.g. Johnson and Smith 1986) have been reported for Antarctic phytoplankton. Although we know grazing always exists, we have a relatively poor knowledge of the typical or mean grazing rate (Huntley et al. 1991). Estimates of production by krill, the dominant grazer, vary by almost two orders of magnitude (Everson 1977). The  $f$ -ratio is used to estimate the  $\text{NO}_3$  consumption. Varying its value over the range observed (0.3–0.8, Smith and Nelson 1990) compared to holding it constant at 0.5 has little effect on the main conclusion regarding the potential of the ACC to utilize available  $\text{NO}_3$ . The lack of horizontal advection is mitigated by the fortuitous result that station A was located in a persistent eddy. Large portions of the ACC that are not near major frontal boundaries exhibit relatively small horizontal gradients, hence the one-dimensional assumption may be reasonable for these regions.

### Conclusions

Based on climatological and observational forcing of a simple one-dimensional ecosystem model, we conclude that utilization

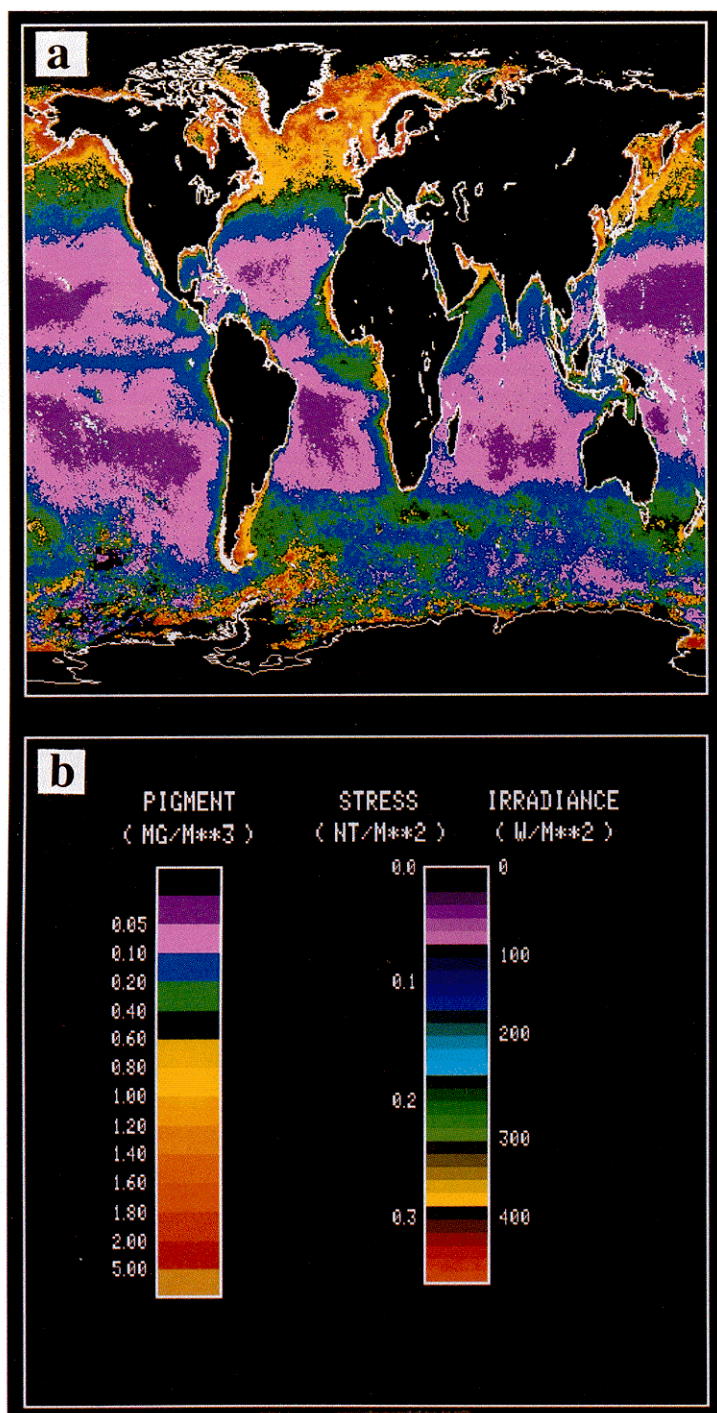


Fig. 7. [a.] Seven-year mean pigment fields derived from the Coastal Zone Color Scanner. [b.] Color bar scaling for panel a and Fig. 8.

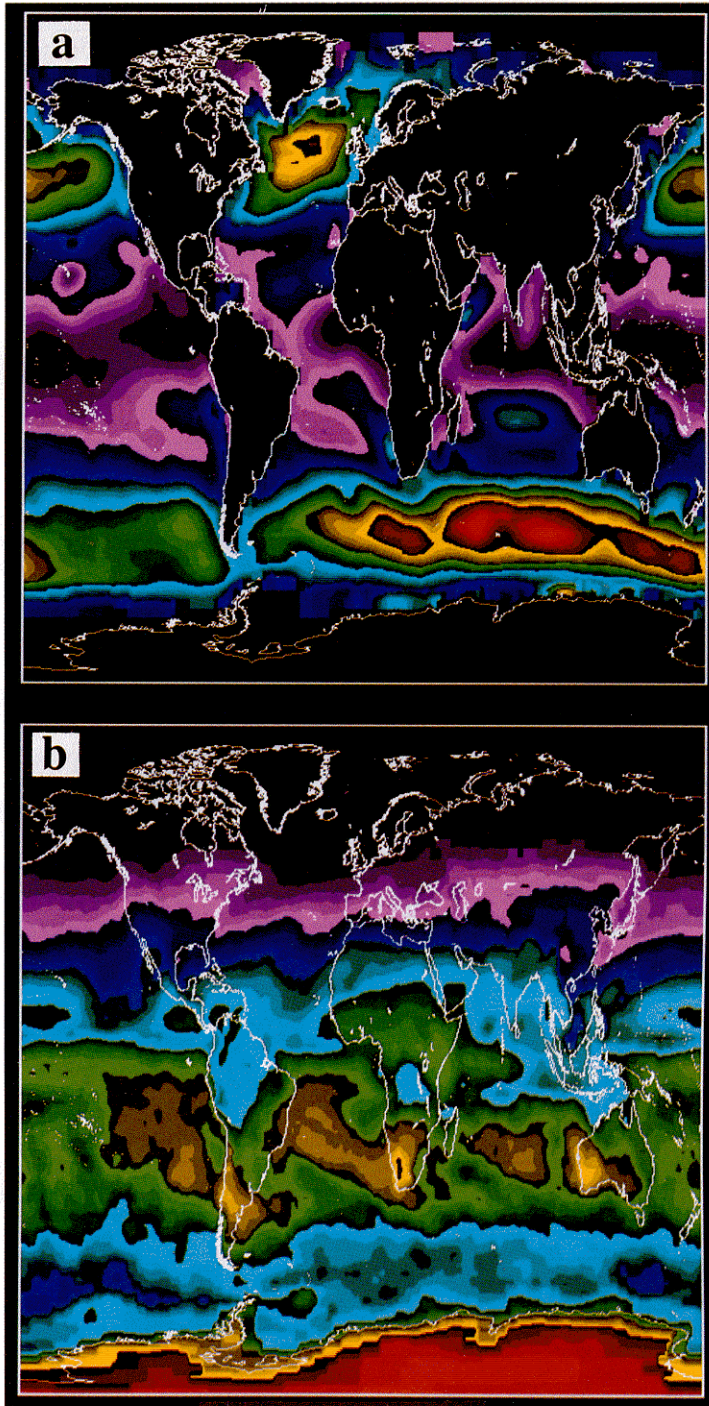


Fig. 8. [a.] Global climatology of annual mean wind stress (from Trenberth et al. 1990). [b.] Global climatology of the monthly surface irradiance for January 1984 (from Bishop and Rossow 1991).

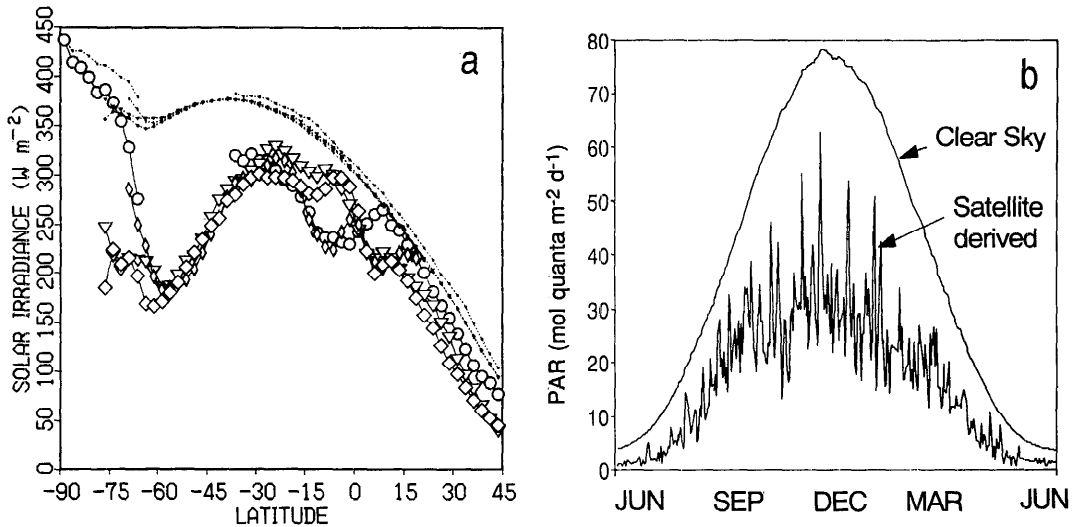


Fig. 9. [a.] Zonal average surface irradiance in January 1984 for land and various ocean basins based on the clear-sky model (small symbols) and satellite-derived estimate (large symbols). (Data from Bishop and Rossow 1991.) [b.] Time series of irradiance at 55°S, 130°W based on the procedure of Bishop and Rossow (1991) for the clear-sky model and satellite-based estimate.

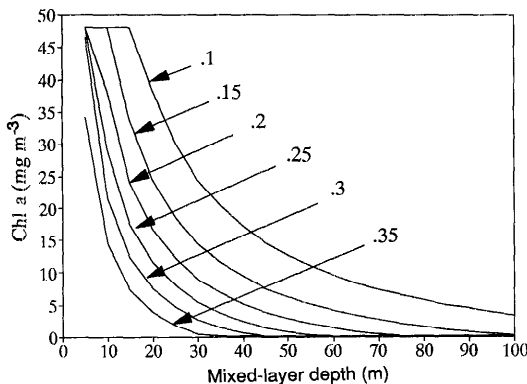


Fig. 10. Prediction of Antarctic phytoplankton crop size on 31 December for various scenarios of mixing and phytoplankton-specific loss rates. For all cases, irradiance was forced with the satellite-derived time series in Fig. 9b. We assume the system cannot attain  $\text{Chl } a > 48 \text{ mg m}^{-3}$  (which is the value that could be attained in an ungrazed "batch" culture with initial  $\text{NO}_3$  concentration of  $30 \text{ mmol m}^{-3}$  C:N ratio of 6.6, and C:Chl *a* ratio of 50. Note that for the typical  $Z_{\text{UML}}$  of 50 m in the ACC, and a loss rate corresponding approximately to respiration alone ( $l = 0.1 \text{ d}^{-1}$ ), only about half of the theoretical maximum crop size would be attained. For a more realistic minimal loss rate ( $0.2 \text{ d}^{-1}$ ), the crop is of the order of 10–20% the maximum. The fraction of available nutrients actually consumed will depend on the rate of resupply from below the euphotic zone and the rate of export of organic matter.

of surface nutrients by phytoplankton in the ACC requires shallower, more stable mixed layers than are observed under present conditions. The model predicts only ~10% of the available nutrients would be utilized for typical physical climatological conditions in the ACC, loss rates that are considered minimal, and reasonable vertical eddy diffusivity coefficients. The precise fraction of nutrients that can be utilized is highly dependent on both biological and physical parameters that determine the aggregate loss rate and vertical supply of deep ocean nutrients, respectively. These terms are poorly characterized and future work must include detailed studies of biological processes, including phytoplankton respiration as a function of irradiance, sinking rates, and grazing rates. Simultaneous studies of physical mixing rates, hydrography, and insolation are required to define in situ irradiance levels and rates of nutrient supply to the euphotic zone. Finally, studies of what limits the phytoplankton crop size for the ACC must also be carried out with simultaneous assessment of the rate of supply and absolute concentrations of trace metals in the euphotic zone and the community response to these concentrations. Answers to



the question at hand will be attained only with a carefully planned interdisciplinary field program that addresses all of these issues simultaneously.

## References

- AUSTIN, R. W. 1974. Inherent spectral radiance signatures of the ocean surface, p. 1–20. *In* S. W. Duntley et al. [eds.], *Ocean color analysis*. Univ. Calif., San Diego SIO Ref. 74-10.
- BARTZ, R., J. R. V. ZANEVELD, AND H. PAK. 1978. A transmissometer for profiling and moored observations in water, p. 102–108. *In* *Ocean optics 5*, Proc. SPIE 160.
- BIGGS, D. C., M. A. JOHNSON, R. R. BIDIGARE, J. D. GUFFY, AND O. HOLM-HANSEN. 1982. Shipboard autoanalyzer studies of nutrient chemistry, 0–200 m, in the eastern Scotia Sea during FIBEX (January–March, 1981). Texas A&M Univ., Dep. Oceanogr. Tech. Rep. 88-11-T.
- BISHOP, J. K. B., AND W. B. ROSSOW. 1991. Spatial and temporal variability of global surface solar irradiance. *J. Geophys. Res.* 96: 16,839–16,858.
- BRIGHTMAN, R. I., AND W. O. SMITH. 1989. Photosynthesis-irradiance relationships of Antarctic phytoplankton during austral winter. *Mar. Ecol. Prog. Ser.* 53: 143–151.
- BUMA, A. G. J., H. J. W. DE BAAR, R. F. NOLTING, AND A. J. VAN BENNEKOM. 1991. Metal enrichment experiments in the Weddell-Scotia Seas: Effects of iron and manganese on various plankton communities. *Limnol. Oceanogr.* 36: 1865–1878.
- BURKHOLDER, P. R., AND E. F. MANDELLI. 1965. Carbon assimilation of marine phytoplankton in Antarctica. *Proc. Natl. Acad. Sci.* 54: 437–444.
- CLARK, A., L. J. HOLMES, AND M. G. WHITE. 1988. The annual cycle of temperature, chlorophyll and major nutrients at Signy Island, South Orkney Islands, 1969–82. *Br. Antarct. Surv. Bull.* 80: 65–86.
- CUSHING, D. H. 1962. An alternative method of estimating the critical depth. *J. Cons. Cons. Int. Explor. Mer* 27: 131–140.
- DE ANGELIS, M., N. I. BARKOV, AND V. N. PETROV. 1987. Aerosol concentrations over the last climatic cycle (160 kyr) from an Antarctic ice core. *Nature* 325: 318–321.
- DE BAAR, H. J. W., AND OTHERS. 1990. On iron limitation in the Southern Ocean: Experimental observations in the Weddell and Scotia Seas. *Mar. Ecol. Prog. Ser.* 65: 105–122.
- DENMAN, K. L. 1973. A time-dependent model of the upper ocean. *J. Phys. Oceanogr.* 3: 173–184.
- , AND A. E. GARGETT. 1983. Time and space scales of vertical mixing and advection of phytoplankton in the upper ocean. *Limnol. Oceanogr.* 28: 801–815.
- , AND M. MIYAKE. 1973. Behavior of the mean wind, the drag coefficient, and the wave field in the open ocean. *J. Geophys. Res.* 78: 1917–1931.
- DUCE, R. A. 1986. The impact of atmospheric nitrogen, phosphorus and iron species on marine biological productivity, p. 497–529. *In* P. Buat-Ménard [ed.], *The role of air-sea exchange in geochemical cycling*. Reidel.
- EL-SAYED, S. Z. 1978. Primary productivity and estimates of potential yields of the Southern Ocean, p. 141–160. *In* M. A. McWhinnie [ed.], *Polar research: To the present and the future*. Westview.
- . 1987. Biological production of Antarctic waters: Present paradoxes and emerging paradigms, p. 1–21. *In* SCAR, *Antarctic aquatic biology*. Biomass Sci. Ser. V. 7. Scott Polar Res. Inst.
- , D. BIGGS, AND O. HOLM-HANSEN. 1983. Phytoplankton standing crop, primary productivity and near-surface nitrogenous nutrient fields in the Ross Sea, Antarctica. *Deep-Sea Res.* 30: 1017–1032.
- EPPLEY, R. W. 1972. Temperature and phytoplankton growth in the sea. *Fish. Bull.* 70: 1063–1085.
- EVERSON, I. 1977. The living resources of the Southern Ocean. FAO.
- FELDMAN, G., AND OTHERS. 1989. Ocean color: Availability of the global data set. *Eos* 70: 634–635, 640–641.
- FOSTER, T. D., AND J. H. MIDDLETON. 1984. The oceanographic structure of the eastern Scotia Sea—1. Physical oceanography. *Deep-Sea Res.* 31: 529–550.
- GLIBERT, P. M., D. BIGGS, AND J. J. MCCARTHY. 1982. Utilization of ammonium and nitrate during austral summer in the Scotia Sea. *Deep-Sea Res.* 29: 837–850.
- GRAN, H. H., AND T. BRARUUD. 1935. A quantitative study of the phytoplankton in the Bay of Fundy and the Gulf of Maine. *J. Biol. Bd. Can.* 1: 279–467.
- GREGG, M. C. 1987. Diapycnal mixing in the thermocline: A review. *J. Geophys. Res.* 92: 5249–5286.
- HART, T. J. 1934. On the phytoplankton of the southwest Atlantic and Bellingshausen Sea, 1929–31. *Discovery Rep.* 8: 1–268.
- HOLM-HANSEN, O., S. Z. EL-SAYED, G. A. FRANCESCHINI, AND R. L. CUHEL. 1977. Primary production and the factors controlling phytoplankton growth in the Southern Ocean, p. 11–50. *In* G. A. Llano [ed.], *Adaptations within Antarctic ecosystems*. Gulf.
- , C. J. LORENZEN, R. W. HOLMES, AND J. D. H. STRICKLAND. 1965. Fluorometric determination of chlorophyll. *J. Cons. Cons. Int. Explor. Mer* 30: 3–15.
- , AND B. G. MITCHELL. 1991. Spatial and temporal distribution of phytoplankton and primary production in the western Bransfield Strait region. *Deep-Sea Res.* 38: 961–980.
- , C. D. HEWES, AND D. M. KARL. 1989. Phytoplankton blooms in the vicinity of Palmer Station, Antarctica. *Polar Biol.* 10: 49–57.
- , AND B. RIEMANN. 1978. Chlorophyll *a* determination: Improvements in methodology. *Oikos* 30: 438–447.
- , L. M. TUPAS, AND I. KOIKE. 1990. RACER: Uptake rates of ammonium and nitrate by phytoplankton populations during the 1989 austral spring bloom. *Antarct. J. U.S.* 25: 154–155.

- , AND M. VERNET. 1990. RACER: Phytoplankton distribution and rates of primary production during the austral spring bloom. *Antarct. J. U.S.* **25**: 141–144.
- HUNTLEY, M. E., D. M. KARL, P. NILER, AND O. HOLM-HANSEN. 1991. Research on Antarctic Coastal Ecosystem Rates (RACER): An interdisciplinary field experiment. *Deep-Sea Res.* **38**: 911–941.
- , AND OTHERS. 1990. RACER: An interdisciplinary study of spring bloom dynamics. *Antarct. J. U.S.* **25**: 126–128.
- JOHNSON, T. O., AND W. O. SMITH. 1986. Sinking rates of phytoplankton assemblages in the Weddell Sea marginal ice zone. *Mar. Ecol. Prog. Ser.* **33**: 131–137.
- KOIKE, I., O. HOLM-HANSEN, AND D. C. BIGGS. 1986. Inorganic nitrogen metabolism by Antarctic phytoplankton with special reference to ammonium cycling. *Mar. Ecol. Prog. Ser.* **30**: 105–116.
- KRAUS, E. B., AND J. S. TURNER. 1967. A one-dimensional model of the seasonal thermocline. 2. The general theory and its consequences. *Tellus* **19**: 98–105.
- LEVITUS, S. 1982. Climatological atlas of the world ocean. NOAA Prof. Pap. 13. U.S. Dep. Commerce.
- MANDELLI, E. F., AND P. R. BURKHOLDER. 1966. Primary productivity in the Gerlache and Bransfield Straits of Antarctica. *J. Mar. Res.* **24**: 15–27.
- MARTIN, J. H. 1990. Glacial-interglacial CO<sub>2</sub> change: The iron hypothesis. *Paleoceanography* **5**: 1–13.
- , S. E. FITZWATER, AND R. M. GORDON. 1990a. Iron deficiency limits growth in Antarctic waters. *Global Biogeochem. Cycles* **4**: 5–12.
- , R. M. GORDON, AND S. E. FITZWATER. 1990b. Iron in Antarctic waters. *Nature* **345**: 156–158.
- MITCHELL, B. G., AND O. HOLM-HANSEN. 1991a. Observations and modeling of the Antarctic phytoplankton crop in relation to mixing depth. *Deep-Sea Res.* **38**: 981–1007.
- , AND ———. 1991b. Bio-optical properties of Antarctic waters: Differentiation from temperate ocean models. *Deep-Sea Res.* **38**: 1009–1028.
- NELSON, D. M., AND W. O. SMITH, JR. 1986. Phytoplankton bloom dynamics of the western Ross Sea ice-edge. 2. Mesoscale cycling of nitrogen and silicon. *Deep-Sea Res.* **33**: 1389–1412.
- , AND ———. 1991. Sverdrup revisited: Critical depths, maximum chlorophyll levels, and the control of Southern Ocean productivity by the irradiance-mixing regime. *Limnol. Oceanogr.* **36**: 1650–1661.
- , AND OTHERS. 1989. Particulate matter and nutrient distributions in the ice-edge zone of Weddell Sea: Relationship to hydrography during late summer. *Deep-Sea Res.* **36**: 191–209.
- NEORI, A., AND O. HOLM-HANSEN. 1982. Effect of temperature on rate of photosynthesis in Antarctic phytoplankton. *Polar Biol.* **1**: 33–38.
- NILER, P. 1975. Deepening of the wind-mixed layer. *J. Mar. Res.* **33**: 405–422.
- , J. ILLEMAN, AND J.-H. HU. 1990. Lagrangian drifter observations of surface circulation in the Gerlache and Bransfield Straits. *Antarct. J. U.S.* **25**: 134–137.
- OLSON, R. J. 1980. Nitrate and ammonium uptake in Antarctic waters. *Limnol. Oceanogr.* **25**: 1064–1074.
- PENG, T.-H., AND W. S. BROECKER. 1990. Dynamical limitations on the Antarctic fertilization strategy. *Nature* **349**: 227–229.
- PLATT, T., K. L. DENMAN, AND A. D. JASSBY. 1977. Modeling the productivity of phytoplankton, p. 807–856. *In* E. D. Goldberg et al. [eds.], *The sea*. V. 6. Wiley.
- , AND A. D. JASSBY. 1976. The relationship between photosynthesis and light for natural assemblages of coastal marine phytoplankton. *J. Phycol.* **12**: 421–430.
- PRISCU, J. C., A. C. PALMISANO, L. R. PRISCU, AND C. W. SULLIVAN. 1989. Temperature dependence of inorganic nitrogen uptake and assimilation in Antarctic sea-ice microalgae. *Polar Biol.* **9**: 443–446.
- REDFIELD, A. C., B. H. KETCHUM, AND F. A. RICHARDS. 1963. The influence of organisms on the composition of sea water, p. 26–77. *In* M. N. Hill [ed.], *The sea*. Interscience.
- RYTHER, J. H., AND C. S. YENTSCH. 1957. The estimation of phytoplankton production in the ocean from chlorophyll and light data. *Limnol. Oceanogr.* **2**: 281–286.
- SAKSHAUG, E., AND O. HOLM-HANSEN. 1986. Photoadaptation in Antarctic phytoplankton: Variations in growth rate, chemical composition and *P* versus *I* curves. *J. Plankton Res.* **8**: 459–473.
- SARMIENTO, J. L., AND U. SIEGENTHALER. 1991. Estimates of the effect of Southern Ocean iron fertilization on atmospheric CO<sub>2</sub> concentrations. *Nature* **349**: 772–775.
- SMETACEK, V., AND U. PASSOW. 1990. Spring bloom initiation and Sverdrup's critical depth model. *Limnol. Oceanogr.* **35**: 228–233.
- SMITH, W. O., AND D. M. NELSON. 1985. Phytoplankton bloom produced by a receding ice edge in the Ross Sea: Spatial coherence with the density field. *Science* **210**: 163–166.
- , AND ———. 1990. Phytoplankton growth and new production in the Weddell Sea marginal ice zone in the austral spring and autumn. *Limnol. Oceanogr.* **35**: 809–821.
- SPIES, A. 1987. Growth rates of Antarctic marine phytoplankton in the Weddell Sea. *Mar. Ecol. Prog. Ser.* **41**: 267–274.
- STEELE, J. H. 1962. Environmental control of photosynthesis in the sea. *Limnol. Oceanogr.* **7**: 137–149.
- , AND D. W. MENZEL. 1962. Conditions for maximum primary production in the mixed layer. *Deep-Sea Res.* **9**: 39–49.
- STRICKLAND, J. D. H., AND T. R. PARSONS. 1972. A practical handbook of seawater analysis, 2nd ed. *Bull. Fish. Res. Bd. Can.* **167**.
- SVERDRUP, H. U. 1953. On conditions for the vernal blooming of phytoplankton. *J. Cons. Cons. Int. Explor. Mer* **18**: 287–295.
- TILZER, M. M., AND Z. DUBINSKY. 1987. Effects of

- temperature and day length on the mass balance of Antarctic phytoplankton. *Polar Biol.* **7**: 35–42.
- TRENBERTH, K. E., W. G. LARGE, AND J. G. OLSON. 1990. The mean annual cycle in global ocean wind stress. *J. Phys. Oceanogr.* **20**: 1742–1760.
- WILSON, D. L., W. O. SMITH, AND D. M. NELSON. 1986. Phytoplankton bloom dynamics of the western Ross Sea ice edge. 1. Primary productivity and species-specific production. *Deep-Sea Res.* **33**: 1375–1387.
- YENTSCH, C. S. 1981. Vertical mixing, a constraint to primary production: An extension of the concept of an optimal mixing zone. *Ecohydrodynamics* **32**: 67–78.